

# Theoretical Studies of the Bonding in Cationic Ruthenium Silylenes

Frederick P. Arnold, Jr.

Advanced Technology Center for Molecular Research, University of Chicago,  
5640 S. Ellis Avenue, Chicago, Illinois 60637

Received July 15, 1999

Hybrid Hartree–Fock/DFT calculations were performed on several model complexes of the general formula  $\text{CpL}_2\text{Ru}=\text{SiX}_2^+$  ( $\text{L} = \text{PH}_3, \text{PMe}_3, \text{CO}, \text{X} = \text{H}, \text{Me}, \text{SH}$ ) as well as  $\text{Cp}(\text{PH}_3)_2\text{Ru}=\text{CH}_2^+$  and analyzed through the use of NBO, CDA, and properties of atoms in molecules. Silicon to ruthenium multiple bonds of low order were found in all of the examined complexes with the exception of  $\text{Cp}(\text{PH}_3)_2\text{RuSi}(\text{SH})_2^+$ . Multiple bonding in these complexes is strengthened through the use of trialkylphosphine ligands on the ruthenium and weakened through the use of  $\pi$ -acids on the ruthenium or substituents other than hydrogen on the silicon. Suggested formulations for improving the  $\pi$ -system are presented.

## Introduction

Transition metal silylene complexes have been an important area of study for several years. Their utility in organosilane polymerization reactions,<sup>1</sup> postulated role as reaction intermediates,<sup>2</sup> and existence as proof of trapping of free, stable, silylenes from solution<sup>3</sup> has caught the interest of many researchers. Isolation has been difficult. Several base-stabilized species have been isolated and represent the majority of the known species,<sup>4</sup> but only a few without<sup>5</sup> coordinating solvent are known. Complexes without external or internal Lewis base stabilization were only recently synthesized by Tilley and co-workers and remain difficult to isolate.<sup>5b,c</sup> This leads one to ask why their isolation has been so difficult, especially in light of the rich and varied carbene<sup>6</sup> and analogous phosphorus<sup>7</sup> chemistry known in the literature.<sup>8</sup>

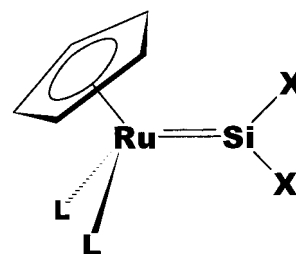


**Figure 1.** Generalized structure of a  $\text{CpL}_2\text{Ru}-\text{SiY}_2^+$  complex.

Complexes of the type  $\text{CpL}_2\text{Ru}=\text{SiY}_2^+$ ,  $\text{L} = (\text{PH}_3, \text{PMe}_3, \text{CO})$ ,  $\text{X} = (\text{H}, \text{Me}, \text{SH})$  (Figure 1), as well as  $\text{Cp}(\text{PH}_3)_2\text{Ru}=\text{CH}_2^+$ , which are models for complexes synthesized by Tilley and co-workers, and the free  $\text{Si}(\text{SH})_2$  ligand were therefore chosen to be examined by both population-based methods (natural bond order, NBO) and charge density analysis (CDA)<sup>9</sup> as well as through examining the topological properties of the electron density (atoms-in-molecules, AIM) in an attempt to obtain a thorough understanding of the nature of the Ru to Si bond.

## Background

There are two basic descriptions of multiple bonding available in these systems. In the traditional Dewar–

(1) (a) Veghini, D.; Henling, L. M.; Burkhardt, T. J.; Bercaw, J. E. *J. Am. Chem. Soc.* **1999**, *121*, 564. (b) Yoshida, T.; Koga, N.; Morokuma, K. *Organometallics* **1996**, *15*, 766. (c) Kunai, A.; Toyoda, E.; Nagamoto, I.; Horio, T.; Ishikawa, M. *Organometallics* **1996**, *15*, 75.

(2) (a) Mitchell, G. P.; Tilley, T. D. *J. Am. Chem. Soc.* **1998**, *120*, 7635. (b) Mitchell, G. P.; Tilley, T. D. *Organometallics* **1996**, *15*, 3477. (c) Wada, H.; Tobita, H.; Ogino, H. *Organometallics* **1997**, *16*, 3970. (d) Tobita, H.; Kurita, H.; Ogino, H. *Organometallics* **1998**, *17*, 2844. (e) Tilley, T. D. in *The Silicon-Heteroatom Bond*; Patai, S., Rappaport, Z., Eds.; Wiley: New York, 1991; Chapters 9 and 10, pp 245 and 309. Lickiss, P. D. *Chem. Soc. Rev.* **1992**, 271. (f) Corey, J. In *Advances in Silicon Chemistry*; Larson, G., Ed.; JAI Press: Greenwich, CT, 1991; Vol. 1, p 327. (g) Pannell, K. H.; Sharma, H. K. *Chem. Rev.* **1995**, *95*, 1351. Zybilla, C. *Top. Curr. Chem.* **1991**, *160*, 1.

(3) (a) Gehrhus, B.; Hitchcock, P. B.; Lappert, M. F.; Maciejewski, H. *Organometallics* **1998**, *17*, 5599. (b) Pannell, K. H.; Sharma, H. K.; Kapoor, R. N.; Cervantes-Lee, F. *J. Am. Chem. Soc.* **1997**, *119*, 9315. (c) West, R.; Denk, M. *Pure Appl. Chem.* **1996**, *68*, 785. (d) Denk, M.; Hayashi, R. K.; West, R. *J. Chem. Soc., Chem. Commun.* **1994**, 33. (e) Jutzi, P.; Möhrke, A. *Angew. Chem., Int. Ed. Engl.* **1990**, *29*, 893.

(4) (a) Ueno, K.; Sakai, M.; Ogino, H. *Organometallics* **1998**, *17*, 2138. (b) Tobita, H.; Kurita, H.; Ogino, H. *Organometallics* **1998**, *17*, 2850. (c) Zybilla, C.; Handwerker, H.; Friedrich, H. In *Advances in Organometallic Chemistry*, vol 36; Academic Press: New York, 1994; p 229, and references therein. (d) Corriu, R. J. P.; Chauhan, B. P. S.; Lanneau, G. F. *Organometallics* **1995**, *14*, 4014. (e) Corriu, R. J. P.; Chauhan, B. P. S.; Lanneau, G. F. *Organometallics* **1995**, *14*, 1646. (f) Chauhan, B. P. S.; Corriu, R. J. P.; Lanneau, G. F.; Priou, C.; Auner, N.; Handwerker, H.; Herdtweck, E. *Organometallics* **1995**, *14*, 1657. (g) Grumbine, S. K.; Straus, D. A.; Tilley, T. D.; Rheingold, A. L. *Polyhedron* **1995**, *14*, 127.

(5) (a) Grumbine, S. K.; Mitchell, G. P.; Straus, D. A.; Tilley, T. D. *Organometallics* **1998**, *17*, 5607. (b) Feldman, J. D.; Mitchell, G. P.; Nolte, J.-O.; Tilley, T. D. *J. Am. Chem. Soc.* **1998**, *120*, 11184. (c) Grumbine, S. K.; Tilley, T. D.; Arnold, F. P.; Rheingold, A. L. *J. Am. Chem. Soc.* **1994**, *116*, 5495. (d) Grumbine, S. D.; Tilley, T. D.; Arnold, F. P.; Rheingold, A. L. *J. Am. Chem. Soc.* **1993**, *115*, 7884. (e) Denk, M.; Hayashi, R. K.; West, R. *J. Chem. Soc., Chem. Commun.* **1994**, 33. (f) Grumbine, S. D.; Tilley, T. D.; Rheingold, A. L. *J. Am. Chem. Soc.* **1993**, *115*, 358. (g) Straus, D. A.; Zhang, C.; Quimbita, G. E.; Grumbine, S. D.; Heyn, R. H.; Tilley, T. D.; Rheingold, A. L.; Geib, S. J. *J. Am. Chem. Soc.* **1990**, *112*, 2673.

(6) Nugent, W. A.; Mayer, J. M. *Metal–Ligand Multiple Bonds*; Wiley: New York, 1988.

(7) Carbene-like phosphorous ligands are of three types: phosphino ( $=\text{PR}_2^+$ ), phosphinidene ( $=\text{PR}$ ), and phosphido ( $=\text{P}$ ).

(8) (a) Wu, G.; Rovnyak, D.; Johnson, M. J. A.; Zanetti, N. C.; Musaev, D. G.; Morokuma, K.; Schrock, R. R.; Griffin, R. G.; Cummins, C. C. *J. Am. Chem. Soc.* **1996**, *118*, 10654. (b) Wagener, T.; Frenking, G. *Inorg. Chem.* **1998**, *37*, 1805.

(9) (a) Dapprich, S.; Frenking, G. *J. Phys. Chem.* **1995**, *99*, 9352. (b) ftp://ftp.chemie.uni-marburg.de/pub/cda. Version 2.1.

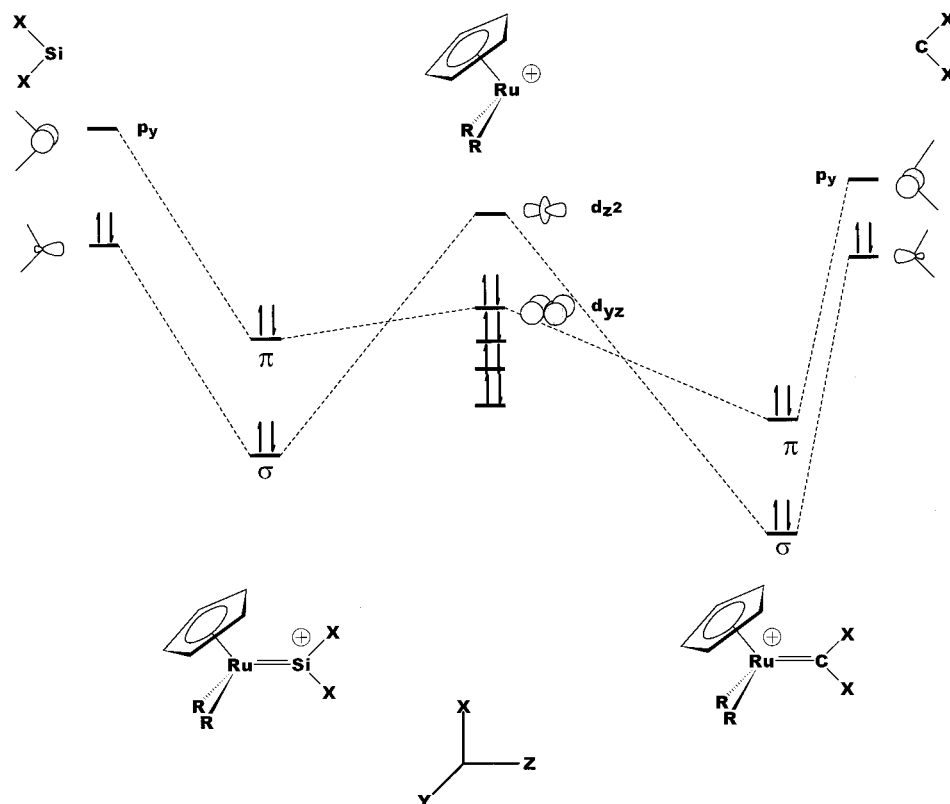


**Figure 2.** Qualitative fragment orbital interaction between a silylene (left) and carbene (right) fragment with a  $\text{CpL}_2\text{Ru}^+$  (center). Note the lesser stabilization of the silylene orbitals vs the carbene and the smaller HOMO–LUMO gap. There exists as well a shift from the positive charge of the system localized on Ru (right) to the charge localized on silicon (left).

Chatt–Duncanson (DCD) model,<sup>10</sup> a closed shell ligand donates an electron pair into a metal-centered acceptor orbital, while the metal back-donates an electron pair into a vacant  $\pi$ -type orbital on the ligand. In this case the carbene is thought of as electrophilic and is generally referred to as a Fischer carbene.<sup>11</sup> The alternative model, in which an alkylidene is formed through a covalent  $\sigma$ - and covalent  $\pi$ -interaction, results in a nucleophilic ligand center. This is often referred to as a Schrock carbene<sup>12</sup> and may be thought of as the other end of a continuum, since a hybrid case possessing a covalent  $\sigma$ -bond, but a  $\pi$ -bond formed through  $d\pi$ – $p\pi$  back-donation is also possible. While these two extremes provide a good theoretical foundation for explaining the bonding situations seen in carbene chemistry, the situation in heavier elements is somewhat less clear-cut.

As was previously shown, the orbital picture is as is shown in Figure 2. These results, derived from Fenske–Hall<sup>13</sup> calculations depict the interaction of a singlet silylene fragment with the  $a$  and  $a'$  frontier orbitals of the  $\text{CpML}_2$  fragment, which leads to a  $\pi$ -bond. When compared with the carbene case, it is noted that both the gap between the  $\sigma$ - and  $\pi$ -systems is smaller and the orbitals are not stabilized as greatly as by the

interaction with the more electronegative carbene fragment. This seems to be at the root of the difficulty in forming silylene to metal multiple bonds: the tendency of the silylene fragment to follow the well-known “diagonal relationship”<sup>14</sup> and act more like an electro-positive borane fragment than a carbene. Therefore, forming a  $\pi$ -bond should be difficult, but forming a  $\sigma$ -bond with a Lewis donor, in the manner of the canonical donor–acceptor complex  $\text{H}_3\text{B}\cdots\text{CO}$ , should be relatively easy. On the other hand, one might retreat to a variation of the old view of bonding in silicon complexes,<sup>15</sup> which is that d-orbital participation leads to some degree of back-bonding from lone-pairs on adjacent atoms. It is not necessary to invoke d-orbitals on silicon in this context,<sup>16</sup> and hence the silylene to Ru system could be thought of as a single bond augmented by  $d\pi$ – $p\pi$  back-bonding, rather than a true double bond.

Results from Fenske–Hall calculations therefore indicated that the base-free complex  $\text{Cp}(\text{PMe}_3)_2\text{Ru}=\text{SiR}_2^+$  should possess a weak silicon to ruthenium double bond,<sup>5c</sup> while the previously isolated platinum complex  $(\text{PCy}_3)_2(\text{H})\text{Pt}=\text{Si}(\text{SEt})_2^+$  was stabilized by intramolecular  $\pi$ -donation from the sulfur ligands and therefore most probably did not possess a multiple bond.<sup>5d</sup> It was

(10) (a) Dewar, M. J. S. *Bull. Chem. Soc. Fr.* **1951**, 18, C79. (b) Chatt, J.; Duncanson, L. A. *J. Chem. Soc.* **1953**, 2929.

(11) Massbol, A.; Fischer, E. O. *Angew. Chem., Int. Ed. Engl.* **1964**, 3, 580.

(12) (a) Schrock, R. R. *J. Am. Chem. Soc.* **1974**, 96, 6796. (b) Taylor, T. E.; Hall, M. B. *J. Am. Chem. Soc.* **1984**, 106, 1576.

(13) (a) Hall, M. B.; Fenske, R. F. *Inorg. Chem.* **1972**, 11, 768. (b) Fenske, R. F.; Caulton, K. G.; Radtke, D. D.; Sweeney, C. C. *Inorg. Chem.* **1966**, 5, 951.

(14) Huheey, J. E. *Principles of Inorganic Chemistry*, 3rd ed.; Harper and Row Publishers: New York, 1987; pp 823–824, 837–839.

(15) Purcell, K. F.; Kotz, J. C. *An Introduction to Inorganic Chemistry*; Saunders College: Philadelphia, PA, 1980; pp 189, 193.

(16) (a) Kutzelnigg, W. *Angew. Chem., Int. Ed. Engl.* **1984**, 23, 272. (b) Reed, A. E.; Weinhold, F. *J. Am. Chem. Soc.* **1986**, 108, 3586. (c) Reed, A. E.; Schleyer, P. v. R. *J. Am. Chem. Soc.* **1990**, 112, 1434. (d) Mollere, P. D.; Hoffmann, R. *J. Am. Chem. Soc.* **1975**, 97, 3680. (e) Cooper, D. L.; Cunningham, T. P.; Gerratt, J.; Karadoakov, P. B.; Raimondi, M. *J. Am. Chem. Soc.* **1994**, 116, 4414.

also determined that, in the case of the ruthenium system, coordination of the silylene fragment to the CpL<sub>2</sub>Ru fragment led to a loss of electron density at the silicon, indicating weak back-bonding. Ab initio and semiempirical calculations by various workers have centered on the Fischer-type silylenes<sup>17</sup> and on hypothetical early metal to silylene systems.<sup>18</sup> Gordon and Cundari studied the unsaturated first-row transition metal to silylene cations, of the form MSiH<sub>2</sub><sup>+</sup>, where M is Sc to Ni.<sup>19</sup> In their study, using the MCSCF/LMO/CI method,<sup>20</sup> it was found that the early metals (Sc–Mn) preferred either a fully covalent description (covalent  $\pi$ - and  $\sigma$ -bonds) or a multiple bond formed by a closed shell donation of an electron pair from the silylene to the metal, to form the  $\sigma$ -bond, and a covalent (shared) interaction to form the  $\pi$ -bond. The late metals, starting with Fe, but especially Co and Ni, preferred a “donor–acceptor” type complex, with two electrons donated from the silylene to the metal to form the  $\sigma$ -bond and two electrons back-donated from the metal to form the  $\pi$ -bond. These latter three had the highest  $\pi$ -bond population and the lowest  $\pi^*$ , giving them the best chance to form stable multiply bonded species, at least with unsaturated metal centers. Ziegler and Jacobsen have estimated that the Fischer-type silylene (CO)<sub>5</sub>Cr=SiCl<sub>2</sub> is stabilized by 22 kcal/mol by the association of phosphine oxide via the unoccupied p-orbital, over the free,  $\pi$ -bound complex. This should be considered a lower bound to the binding energy, since generally these complexes are associated with the much stronger base HMPA (hexamethylphosphoramide). All of the calculations agree that the chief problems in forming the silicon to metal multiple bond is the low electronegativity of the silicon fragment, which leads to weak  $\pi$ -bonds, competition from Lewis bases, and heavy polarization of the bond toward the transition metal. However, in all of the above cases, the metal has had significant electron-withdrawing ability of its own (Cr, Mo, W, with CO ligands), has been an early, electropositive element (Zr, Hf) which has poor donor ability, or has been an unsaturated metal center, which has forced an interaction with the silicon through lack of alternative ligands. It is therefore relevant to investigate the ability of a late, second-row, electron-rich metal center to participate in significant back-bonding, thereby stabilizing a Si–M multiple bond.

To gain a proper understanding of the bonding present in this system, two methods that have proved to be less arbitrary than the traditional Mulliken population based schemes were employed, NBO and atoms-in-molecules.

Natural bond order analysis, the associated natural population analysis, and natural localized molecular orbitals are an orbital population based localization

scheme that attempts to reproduce the best Lewis type structure in term of two electron domains (lone-pairs, three-center–two-electron bonds, and bonds).<sup>21</sup> It has the advantage of transforming the delocalized, canonical, molecular orbitals, which are distributed over the entire molecule, into localized orbitals that represent a more “chemical” view of the system. While not without its difficulties, it has also been shown to be relatively independent of basis set effects that plague the more traditional population analysis methods<sup>22</sup>

The atoms-in-molecules (AIM) analysis method differs from the previously described methods in that it is dependent solely upon the electron density  $\rho$  of the system and so in principle is independent of orbitals and may be applied to experimentally derived data. While traditionally used to explain the bonding in main-group systems, AIM has recently been applied to a variety of transition metal systems with considerable success.<sup>23</sup> The quantities of interest for this study are the curvature of the laplacian and the ellipticity of the critical point. A higher ellipticity is an indication of a preference for charge accumulation within specific regions and indicates either multiple-bond character or “bent” bond character, such as is seen in cyclopropane.<sup>24</sup> Systems in which there exists either a high ellipticity or a small difference between the value of  $\rho$  at bond and neighboring ring critical points are potentially unstable. The sign of the laplacian indicates where charge is either locally accumulated ( $\nabla^2\rho < 0$ ) or depleted ( $\nabla^2\rho > 0$ ) and may be used to distinguish between a covalent interaction ( $\nabla^2\rho < 0$ ) or a “closed shell” (ionic or donor–acceptor) interaction. The AIM method also allows one to define a bond in a physically meaningful fashion, through analysis of the gradient of the electron density,  $\nabla\rho$ . The bond path between two atoms is that line between two nuclei along which the electron density is a local maximum. A (3,–1), or bond, critical point defines the boundary between two adjacent atomic surfaces and represents a local maxima on that surface and a minima along the bond path. A (3,1), or ring, critical point arises when several bond paths are linked into a ring. At the center of the ring will be a point that is a local minima on the ring surface, which is the surface formed by all gradient paths originating at the ring point and ending at the associated bond points. Should several rings be arranged so as to enclose the interior of the molecule, a (3,3), or cage, critical point will be found, where it is a minima in all directions. The corresponding nuclear critical point (3,–3) represents a local maximum, generally coincident with the atomic nuclei.<sup>25</sup>

## Computational Section

Structures were optimized using Gaussian 94 revision E2<sup>26</sup> using the B3PW91 hybrid functional.<sup>27</sup> The basis set employed

(17) (a) Jacobsen, H.; Ziegler, T. *Inorg. Chem.* **1996**, *35*, 775. (b) Jacobsen, H.; Ziegler, T. *Organometallics* **1995**, *14*, 224. (c) Nakatsuji, H.; Ushio, J.; Yonezawa, T. *J. Organomet. Chem.* **1983**, *258*, C1. (d) Abronin, I. A.; Avdyuhina, N. A.; Morozova, L. V.; Magomedov, G. K. *I. J. Mol. Struct. (THEOCHEM)* **1991**, *228*, 19. (e) Marquez, A.; Sanz, J. F. *J. Am. Chem. Soc.* **1992**, *114*, 2903.

(18) Cundari, T. R.; Gordon, M. S. *Organometallics* **1992**, *11*, 3122.

(19) Cundari, T. R.; Gordon, M. S. *J. Phys. Chem.* **1992**, *96*, 631.

(20) (a) Cundari, T. R.; Gordon, M. S. *J. Am. Chem. Soc.* **1991**, *113*, 5231. (b) Feller, D. F.; Schmidt, M. W.; Ruedenberg, K. *J. Am. Chem. Soc.* **1982**, *104*, 960. (c) Ruedenberg, K.; Schmidt, M. W.; Dombek, M. M.; Elbert, S. T. *Chem. Phys.* **1982**, *71*, 41, 51, 65. (d) Lam, B.; Schmidt, M. W.; Ruedenberg, K. *J. Phys. Chem.* **1985**, *89*, 2221.

(21) Reed, A. E.; Curtiss, L. A.; Weinhold, F. *Chem. Rev.* **1988**, *88*, 899.

(22) Lüthi, H. P.; Ammeter, J. H.; Almlöf, J.; Faegri, K., Jr. *J. Chem. Phys.* **1982**, *77*, 2002.

(23) (a) Frenking, G.; Pidun, U. *J. Chem. Soc., Dalton Trans.* **1997**, 1653. (b) Frenking, G.; Vyboishchikov, S. F. *Chem. Eur. J.* **1998**, *4*, 1428. (c) Ehlers, A. W.; Frenking, G.; Baerends, E. J. *Organometallics* **1997**, *16*, 4896. (d) Gillespie, R. J.; Bytheway, I.; Tang, T.-H.; Bader, R. F. W. *Inorg. Chem.* **1996**, *35*, 3954. (e) Lin, Z.; Bytheway, I. *Inorg. Chem.* **1996**, *35*, 594.

(24) Bader, R. F. W. *Atoms in Molecules, a Quantum Theory*; Clarendon Press: Oxford, U.K., 1994.

**Table 1.** CpL<sub>2</sub>Ru=SiX<sub>2</sub><sup>+</sup> Geometrical Parameters

L	X	r(Ru–Si) (Å)	r(Ru–P) (Å)	dihedral (cent–Ru–Si–X) (deg)
PH <sub>3</sub>	H	2.232	2.304	0.0
PH <sub>3</sub>	Me	2.257	2.296	1.5
PH <sub>3</sub>	SH	2.258	2.307	0.0
PMe <sub>3</sub>	H	2.215	2.335	2.8
PMe <sub>3</sub>	Me	2.250	2.330	31.5
CO	H	2.259		0.0
PH <sub>3</sub> <sup>a</sup>	CH <sub>2</sub>		2.304	0.0
PMe <sub>3</sub> <sup>b</sup>	Me	2.2383	2.2915	34.0

<sup>a</sup> Molecule is Cp(PH<sub>3</sub>)<sub>2</sub>Ru=CH<sub>2</sub><sup>+</sup>. r(Ru=C) = 1.8905 Å. <sup>b</sup> Experimental structure: Cp\*(PMe<sub>3</sub>)<sub>2</sub>Ru=SiMe<sub>2</sub>[B(C<sub>6</sub>F<sub>5</sub>)<sub>4</sub>], ref 5c.

for geometry optimization and orbital-based analyses was the LANL2DZ,<sup>28</sup> augmented by polarization functions on the main-group elements, taken from the 6-31G(d) basis set. The values and nature of the exponents were C(d) = 0.80, P(d) = 0.55, Si(d) = 0.395, S(d) = 0.65, O(d) = 0.80.<sup>29</sup> For the AIM analysis single-point calculations were performed using the Huzinaga Ru(7f) basis set with two p-type polarization functions of value 0.030 and 0.091 and with the outermost d-function split into a 2–1 contraction.<sup>30</sup> Basis sets used for the AIM analysis for the main-group elements were the standard 6-311+G\*.<sup>31</sup>

Atoms-in-molecules analysis<sup>32</sup> was performed with the program EXTREME (ext94b) of Professor R. F. W. Bader's AIM-PAC<sup>33</sup> suite of programs and P. Popelier's program MORPHY 1.0.<sup>34</sup> Bond paths were traced to ensure that (3,–1) critical points between atoms connected those atoms.<sup>35</sup> Population-based analyses and NBO analysis were performed with the stand-alone version of NBO 4.0.<sup>36</sup> The program CDA2.1 by Frenking and Dapprich was used to investigate the donor–acceptor nature of the complexes.<sup>8</sup> Visualization was performed using WebLab Viewer Pro v. 3.2<sup>37</sup> and Spartan 5.1.<sup>38</sup>

## Results

Geometrical results are presented in Table 1. It is immediately apparent that despite the differing substituents, the Ru–Si bond distances fall within a fairly narrow interval, from 2.215 to 2.259 Å, with the

complexes with L = CO, X = H and L = PH<sub>3</sub>, X = SH possessing the longest bond distances. These distances are in good agreement with the isolated, base-free structure [Cp\*(PMe<sub>3</sub>)<sub>2</sub>Ru=SiMe<sub>2</sub>][B(C<sub>6</sub>F<sub>5</sub>)<sub>4</sub>], which possesses a Ru–Si bond distance of 2.238 Å. The observed distances are also all slightly shorter than those found in (Me<sub>3</sub>P)<sub>2</sub>RuSi[S(*p*-tolyl)]Os(CO)<sub>4</sub> (2.2862 Å)<sup>39</sup> and (Me<sub>3</sub>P)<sub>2</sub>RuSi[S(*p*-tolyl)](phen)<sub>2</sub><sup>+</sup> (2.2695 Å).<sup>40</sup> The shortest bond belongs to the complex Cp(PMe<sub>3</sub>)<sub>2</sub>Ru=SiH<sub>2</sub><sup>+</sup>, while moving the methyl group to the silicon causes a lengthening to 2.2568 Å. This trend is not uniform with the L = PMe<sub>3</sub>, X = Me system displaying a bond almost as long (2.250 Å). There is little pattern seen in the Ru–P bond distances, and it seems to correlate better with the type of phosphine than the Ru–Si bond distance.

Most complexes displayed the theoretically preferred Cp(centroid)–Ru–Si–X dihedral angle of 0°, as opposed to the experimentally observed twisted geometries. The exceptions were observed when methyl groups were added to either the phosphine ligands or the silylene. With R = PMe<sub>3</sub>, X = H, a twist of just over 2° was observed. When methyl groups were added to the silicon as well, the twist increased to 31°, which is close to the experimentally observed twist of 34° observed in Cp\*(PMe<sub>3</sub>)<sub>2</sub>Ru=SiMe<sub>2</sub><sup>+</sup>. Methyl groups on the silicon alone led to a twist of 1.5°, as well as an increase in the RuSi bond length by 0.025 Å. The twisted geometry is therefore thought to arise primarily from steric effects. The experimentally characterized systems are based upon the bulkier Cp\* ligand, which increases the steric bulk about the ruthenium, and the deviation from the ideal structure.<sup>41</sup> We will return to this issue in the Discussion.

The bond paths, as shown in Figure 3, trace a molecular framework that one would expect on the basis of Lewis structures. Attention is immediately drawn to the Cp–M bonds, in which the picture is that of one C–M bond for each member of the Cp ring, as opposed to one bond to the Cp centroid. Also present are C–Ru–C ring critical points<sup>42</sup> between each two C's and the central metal and the existence of a (3,3) cage critical point in the center of the Cp–Ru moiety.<sup>43</sup>

Only two deviations from this picture exist: in the case of Cp(PH<sub>3</sub>)<sub>2</sub>Ru=CH<sub>2</sub><sup>+</sup>, the Cp carbon in the H–C–Ru plane does not show a bond, although the other four carbons in the Cp ring form Ru–C bonds, and in the case of Cp(PMe<sub>3</sub>)<sub>2</sub>Ru=SiH<sub>2</sub><sup>+</sup>, there are two strongly curved bond paths that connect Cp hydrogens and methyl hydrogens and only three Cp–Ru bonds. In the former case, as shown in Table 2, there is a (3,+1) ring critical point instead of the expected (3,–1). The missing

(25) Ref 24, pp 28–39, and ref 34.

(26) Frisch, M. J.; Trucks, G. W.; Schlegel, H. B.; Gill, P. M. W.; Johnson, B. G.; Robb, M. A.; Cheeseman, J. R.; Keith, T.; Petersson, G. A.; Montgomery, J. A.; Raghavachari, K.; Al-Laham, M. A.; Zakrzewski, V. G.; Ortiz, J. V.; Foresman, J. B.; Cioslowski, J.; Stefanov, B. B.; Nanayakkara, A.; Challacombe, M.; Peng, C. Y.; Ayala, P. Y.; Chen, W.; Wong, M. W.; Andres, J. L.; Replogle, E. S.; Gomperts, R.; Martin, R. L.; Fox, D. J.; Binkley, J. S.; Defrees, D. J.; Baker, J.; Stewart, J. P.; Head-Gordon, M.; Gonzalez, C.; Pople, J. A. *Gaussian 94, Revision E.2*; Gaussian, Inc.: Pittsburgh, PA, 1995.

(27) Becke, A. D. *J. Chem. Phys.* **1993**, *98*, 5648.

(28) (a) Hay, P. J.; Wadt, W. R. *J. Chem. Phys.* **1985**, *82*, 270. (b) Hay, P. J.; Wadt, W. R. *J. Chem. Phys.* **1985**, *82*, 284. (c) Hay, P. J.; Wadt, W. R. *J. Chem. Phys.* **1985**, *82*, 299.

(29) Note: the value of the d-function on silicon (0.395) is not the standard 6-31G\* value, but an improved one from: Gordon, M. S. *Chem. Phys. Lett.* **1980**, *76*, 163.

(30) Huzinaga, S., et al., Eds.; *Gaussian Basis Sets for Molecular Calculations*; Elsevier Science Publishers B. V.: Amsterdam, The Netherlands, 1984.

(31) Krishnan, R.; Binkley, J. S.; Seeger, R.; Pople, J. A. *J. Chem. Phys.* **1980**, *72*, 650.

(32) Wiberg, K. B.; Bader, R. F. W.; Lau, C. D. H. *J. Am. Chem. Soc.* **1987**, *109*, 985.

(33) Available in source form (F77) from <http://www.chemistry.mcmaster.ca/aimpac>.

(34) Popelier, P. L. A. *Comput Phys. Commun.* **1996**, *93*, 212.

(35) Bader, R. F. W. *J. Phys. Chem. A* **1998**, *102*, 7314

(36) Glendening, E. D.; Badenhoop, J. K.; Reed, A. E.; Carpenter, J. E.; Weinhold, F. *NBO 4.0*; Theoretical Chemistry Institute, University of Wisconsin: Madison, WI, 1996.

(37) WebLab Viewer Pro, from MSI Inc., 9685 Scranton Road, San Diego, CA 92121-3752, a subsidiary of Pharmacoepia, Inc.

(38) *Spartan 5.1*; Wavefunction Inc.: 18401 Von Karman Ave., Ste. 370, Irvine, CA 92612.

(39) Grumbine, S. D.; Tilley, T. D.; Rheingold, A. L. *J. Am. Chem. Soc.* **1993**, *115*, 358.

(40) Grumbine, S. D.; Chadha, R. K.; Tilley, T. D. *J. Am. Chem. Soc.* **1992**, *114*, 1518.

(41) Albright, T. A.; Burdett, J. K.; Whangbo, M.-H., *Orbital Interactions in Chemistry*; Wiley-Interscience: New York, 1985; pp 397–398.

(42) A critical point is a region where the curvature of the electron density is a local maxima or minima. See refs 32 and 24 for more details.

(43) The cage critical point, a region of local electron depletion, leads to a model of Cp–M binding being roughly cone-shaped, originating at the metal and extending to the ring carbons. This is mostly in accord with the orbital view that envisions the π-electron ring interacting with the metal, but with a more localized character; that is, definite C–M bonds exist, rather than a completely delocalized interaction.

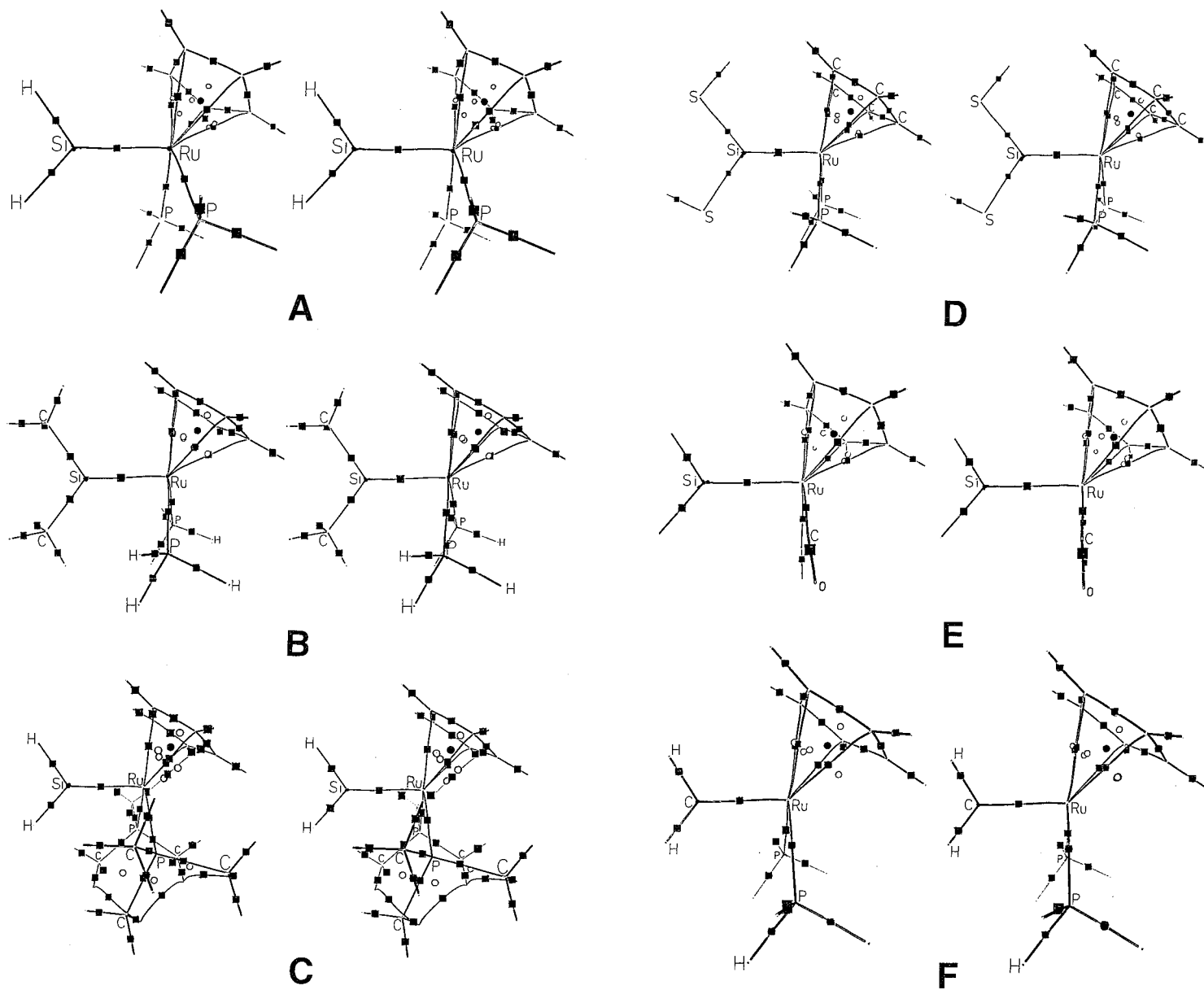


**Figure 3.** Relaxed eye stereopairs of the molecular graphs of the molecules in the article. Some labels have been omitted for clarity. Bond paths (black lines), bond critical points (black squares), ring critical points (open circles), and cage critical points (filled circles) are shown for (a)  $\text{Cp}(\text{PH}_3)_2\text{RuSiH}_2^+$ , (b)  $\text{Cp}(\text{PH}_3)_2\text{RuSiMe}_2^+$ , (c)  $\text{Cp}(\text{PMe}_3)_2\text{-RuSiH}_2^+$ , (d)  $\text{Cp}(\text{PH}_3)_2\text{RuSi}(\text{SH})_2^+$ , (e)  $\text{Cp}(\text{CO})_2\text{RuSiH}_2^+$ , and (f)  $\text{Cp}(\text{PH}_3)_2\text{RuCH}_2^+$ .  $\text{Cp}(\text{PMe}_3)_2\text{RuSiMe}_2^+$  has been omitted for clarity, but is similar to  $\text{Cp}(\text{PMe}_3)_2\text{RuSiH}_2^+$ .

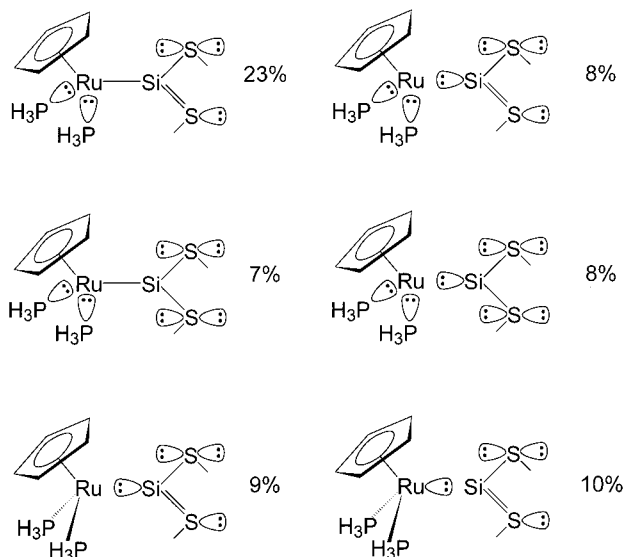


**Figure 4.** NRT resonance weights of the most highly weighted configurations for  $\text{Cp}(\text{PH}_3)_2\text{Ru}-\text{Si}(\text{SH})_2^+$ .

**Table 2.** Cp(C)–Ru Bond Lengths, Critical Points, Electron Density ( $\rho$ ), and Ellipticity ( $\epsilon$ )

L	X	$r(\text{Ru}-\text{C})$	CP <sup>a</sup>	$\rho$	$\epsilon$
PH <sub>3</sub>	SiH <sub>2</sub>	2.270	B	0.0715	1.54
		2.269	B	0.0709	3.49
		2.269	B	0.0709	3.48
		2.270	B	0.0716	1.54
		2.297	B	0.0671	9.86
PH <sub>3</sub>	SiMe <sub>2</sub>	2.303	B	0.0662	14.4
		2.273	B	0.0710	1.65
		2.267	B	0.0712	3.24
		2.267	B	0.0712	3.21
		2.272	B	0.0712	1.60
PH <sub>3</sub>	Si(SH) <sub>2</sub>	2.264	B	0.0717	2.98
		2.266	B	0.0720	1.73
		2.277	B	0.0694	4.71
		2.266	B	0.0720	1.73
		2.264	B	0.0717	2.98
PMe <sub>3</sub>	SiH <sub>2</sub>	2.269	B	0.0714	1.30
		2.275	B	0.0705	2.07
		2.313	B	0.0656	2.88
		2.320	R	0.0629	N/A
		2.293	N	N/A	N/A
PMe <sub>3</sub>	SiMe <sub>2</sub>	2.305	B	0.0665	1.68
		2.305	B	0.0662	3.65
		2.295	B	0.0670	3.45
		2.302	B	0.0666	2.16
		2.321	B	0.0636	8.85
CO	SiH <sub>2</sub>	2.304	B	0.0668	8.63
		2.280	B	0.0704	1.85
		2.290	B	0.0693	2.28
		2.281	B	0.0693	3.37
		2.283	B	0.0694	3.23
PH <sub>3</sub>	CH <sub>2</sub>	2.294	B	0.0675	5.46
		2.294	B	0.0675	5.46
		2.287	B	0.0698	1.25
		2.287	B	0.0698	1.25
		2.329	R	0.0630	N/A

<sup>a</sup> R = Ring (3,+1), B = Bond (3,-1), N = No CP on internuclear axis.

bonds arising from the lack of 5-fold symmetry in the bonds is related to local densities arising from orbital effects, as was discussed in earlier work by Marynick.<sup>44</sup> The bond lengths, along with the value of the electron density at the bond critical points, are shown in Table

(44) (a) Marynick, D. S. *J. Am. Chem. Soc.* **1977**, *99*, 1436. (b) Marynick, D. S.; Lipscomb, W. N. *J. Am. Chem. Soc.* **1972**, *94*, 8692.

2. Those carbons with distances from the ruthenium of greater than 2.30 Å do not possess a Ru–C (3,-1) critical point. Each set of five bonds may be divided into three groups, with the longer bonds possessing both a lower value of  $\rho$  at the critical point and a higher ellipticity. In each case one carbon possesses a notably higher value, often by a factor of 3 or more, than the others, and in all cases the ellipticities are an order of magnitude higher than those of the Ru–Si or Ru–P critical points. It should also be noted that at the ring and cage points, while the value of  $\rho$  is a local minima, the absolute value is very similar, being approximately 0.06 e/bohr<sup>3</sup>. The local curvature of the electron density does not correspond to a bond being present, not that the electron density is absent. For comparative purposes, it should be noted that the value of  $\rho$  at the Cp–Ru bond critical points is half that of the Ru–CO bonds. The observed difference in value of the electron density is consistent with the standard view of a Cp ring possessing three distinct orbital configurations ( $e'$ ,  $e''$ , and  $a$ ) and explains the missing critical points previously mentioned. One bond of the manifold is longer than the others, and a minor distortion of the Cp ring causes the bond to rupture and the electron density to redistribute itself accordingly among the remaining bonds. In accordance with previous results, we may therefore expect that these bonds are particularly susceptible to bond rupture or ring-slippage,<sup>45</sup> with this disruption occurring most easily in those complexes that are most electron rich. The question of the two strongly curved paths connecting the ruthenium center to hydrogens on the methyl groups of  $\text{Cp}(\text{PMe}_3)_2\text{Ru}=\text{SiH}_2^+$  and  $\text{Cp}(\text{PMe}_3)_2\text{Ru}=\text{SiMe}_2^+$  is more difficult. These may be artifacts of the calculation or may indicate a weak interaction between hydrogens possessing a small difference in charge. Since AIM is basis set independent and derives only from the properties of the charge density of the system, it is considered that the interaction is probably a real, albeit small, electrostatic one.<sup>46</sup> This mode of bonding will not be considered further in this study, as it does not involve the metal–silicon bonding manifold.

The Ru–Si (3,-1) critical points are mostly unremarkable, being located at the midpoint of the bond and possessing similar values for the charge density and ellipticity. All of the observed critical points demonstrate an ellipticity consistent with some degree of multiple bonding being present, though much lower than observed in ethylene or benzene with basis sets of comparable size. The Si–C bonds are polarized toward the carbon in the manner of the Si–SH bonds in the thiol complex, indicating that the relative electronegativity difference between carbon and silicon is leading to charge depletion at the silicon.<sup>47</sup>

Table 3 shows the difference between the all-electron Huzinaga basis set on Ru and the LANL2DZ effective core potential and associated valence plus 4s,4p basis set. For the purposes of our study, it is important to

(45) Bader, R. F. W. *Atoms in Molecules, a Quantum Theory*; Clarendon Press: Oxford, U.K., 1994; pp 83–85.

(46) Popelier, P. L. A. *J. Phys. Chem. A* **1998**, *102*, 1873.

(47) (a) Pauling electronegativities are as follows: C = 2.55, S = 2.58, Si = 1.90. From: Jolly, W. L. *Modern Inorganic Chemistry*; McGraw-Hill: New York, 1984; p 72. (b) The methyl group is estimated to have an electronegativity of 2.27. Huheey, J. E. *J. Phys. Chem.* **1965**, *69*, 3284.

**Table 3. AIM Results:  $\rho$ ,  $\nabla^2\rho$ ,  $\epsilon$ ,  $E(r)$  at the Ru–Si (3,–1) Critical Point**

L	X	$\rho$ (au/bohr <sup>3</sup> )	$\nabla^2\rho$ (au/bohr <sup>3</sup> )	$\epsilon$	$E(r)$ (au/bohr <sup>3</sup> )
PH <sub>3</sub>	H	$1.001 \times 10^{-1}$	$-2.867 \times 10^{-2}$	$2.510 \times 10^{-2}$	$-5.402 \times 10^{-2}$
PH <sub>3</sub>	Me	$9.804 \times 10^{-2}$	$-2.313 \times 10^{-2}$	$2.551 \times 10^{-1}$	$-5.015 \times 10^{-2}$
PH <sub>3</sub>	SH	$9.391 \times 10^{-2}$	$+2.342 \times 10^{-2}$	$1.510 \times 10^{-1}$	$-4.348 \times 10^{-2}$
PMe <sub>3</sub>	H(Full)	$1.019 \times 10^{-1}$	$-3.453 \times 10^{-2}$	$2.624 \times 10^{-1}$	$-5.715 \times 10^{-2}$
PMe <sub>3</sub>	H(ECP)	$2.082 \times 10^{-1}$	$+6.925 \times 10^{-1}$	$6.580 \times 10^{-2}$	$-16.732 \times 10^{-2}$
PMe <sub>3</sub>	Me	$9.813 \times 10^{-2}$	$-1.493 \times 10^{-2}$	$2.491 \times 10^{-1}$	$-4.978 \times 10^{-2}$
CO	H	$9.820 \times 10^{-2}$	$-3.189 \times 10^{-2}$	$2.182 \times 10^{-1}$	$-5.029 \times 10^{-2}$
PH <sub>3</sub> <sup>a</sup>	CH <sub>2</sub>	$1.708 \times 10^{-1}$	$+2.685 \times 10^{-1}$	$6.880 \times 10^{-2}$	$-9.391 \times 10^{-2}$

<sup>a</sup> Molecule is Cp(PH<sub>3</sub>)<sub>2</sub>Ru=CH<sub>2</sub><sup>+</sup>. Properties are for the Ru–C (3,–1) critical point.

**Table 4. Properties Derived from NBO Analysis**

L	X	bond order (Wiberg)	bond order (NLMO)	NPA charge (Ru)	NPA charge (E)	Ru–E bond pop. (electrons)	pop. in Si lone pair (electrons)
PH <sub>3</sub>	H	0.8822	1.0283	–0.594	0.909 (Si)	1.623 (Si)	0.326
PH <sub>3</sub>	Me	0.7939	0.9525	–0.618	1.459 (Si)	1.785 (Si)	0.313
PH <sub>3</sub>	SH	0.7123	0.8315	–0.604	0.865 (Si)	1.822 (Si)	0.563
PMe <sub>3</sub>	H(0°)	0.9367	1.1443	–0.582	0.865 (Si)	1.809 (Si)	0.374
PMe <sub>3</sub>	H(35°)	0.9254	1.1541	–0.588	0.894 (Si)	1.810 (Si)	0.341
PMe <sub>3</sub>	Me	0.8404	1.0723	–0.606	1.430 (Si)	1.791 (Si)	0.320
CO	H	0.7607	0.8222	–0.396	1.038 (Si)	1.802 (Si)	0.241
PH <sub>3</sub> <sup>a</sup>	CH <sub>2</sub>	1.1965	1.2597	–0.238	–0.234 (C)	3.430 (C)	

<sup>a</sup> Molecule is Cp(PH<sub>3</sub>)<sub>2</sub>Ru=CH<sub>2</sub><sup>+</sup>. NBO reports a covalent double bond, rather than donor–acceptor complex. See text for more details.

note that while the sign of  $\nabla^2\rho$  differs, the values of the energy density  $E(r)$  are very similar and provide a better indicator of closed shell vs covalent character. Interestingly the value of  $\rho$  at the (3,–1) critical point is higher in the ECP case than the all-electron, but the ellipticity is lower. It is believed that this difference in behavior is a result of the lack of Ru core electrons.<sup>48</sup> Bond paths traced using the ECP wave function resulted in spurious critical points and unreasonable bond paths, when compared with the all-electron example. Therefore they were not used further for the AIM analysis. The savings in computational time on this study, where only one second-row transition metal atom is present, is small, but would be important for third-row or for cluster studies involving multiple metal atoms.

The energy difference between the untwisted form of Cp(PMe<sub>3</sub>)<sub>2</sub>Ru=SiH<sub>2</sub><sup>+</sup> and the 35° twisted form, uncorrected for zero-point energies, is 1.67 kcal/mol, in favor of the untwisted geometry. This difference is negligible and reinforces the evidence for a weak  $\pi$ -bond. This is also consistent with the NBO description of the Ru–Si bond, which indicates that upon twisting, the population in the Si lone-pair orbital actually decreases (Table 4). This result contradicts an earlier result at the RHF level of theory<sup>49</sup> which indicated that the twist would lead to a net stabilization due to better population of the vacant p-orbital at silicon. The earlier result is therefore an artifact of an inappropriate level of theory.

NBO results are summarized in Table 4. The canonical NBO structures of the Ru–Si species all consist of a Ru–Si single bond, with the  $\pi$ -bond being formed by donation of a lone-pair on ruthenium into the vacant p-orbital on silicon. The  $\sigma$ -bonds are unremarkable, being formed from approximately equal parts ruthenium and silicon orbitals. The only significant deviation from this form is in the case of Cp(PH<sub>3</sub>)<sub>2</sub>Ru=SiH<sub>2</sub><sup>+</sup>, in which the  $\sigma$ -orbital is 60% silicon and 40% ruthenium.

It is immediately apparent that the highest  $\sigma/\pi$ -bond populations are in the case of L = PMe<sub>3</sub>, X = H,

twist = 0°. An apparent higher population in the case of X = SH is spurious, as a calculation on the free (SH)<sub>2</sub>Si fragment indicates. The Si p-orbital population in the free dithiolsilylene is 0.50 electron, indicating almost no back-bonding from the metal into this fragment. Also apparent is that the natural charges on the silicon are heavily perturbed by the nature of the substituent at silicon, with the dimethylsilyl fragments possessing a charge of 1.4 and the dihydro and dithiol possessing a charge of approximately 0.86. This would indicate that the methyl group is sufficiently electronegative to induce a lower electron population at silicon, leading to weaker donation to the metal center, while lacking the intramolecular Lewis base character of the thiol groups. This effect has been observed previously in the context of saturated metal–silicon systems.<sup>50</sup> Si p-orbital populations are little perturbed by change of substituent, indicating that most of the charge difference arises from perturbation of the  $\sigma$ -framework. The contrast between the ruthenium silylene and ruthenium carbene is striking. In the carbene case the carbon is carrying a strong negative charge (–0.234), and the ruthenium is more electron deficient as well (–0.238), with a combined  $\sigma$ - $\pi$ -orbital population of 3.43 electrons, resulting in a bond order of approximately 1.7. This is in marked contrast to the silylenes, which rarely achieve a total population above 2.2 or a bond order of 1.1. A greater degree of back-bonding exists in the carbene system (approximately 0.3 electron, when compared with the silylene average), despite the  $\sigma$ -orbital population of 1.760 electrons, which is slightly lower than the mean of the silicon–ruthenium populations. The high bond order is despite the use of the PH<sub>3</sub> group on the metal center, which in the silylene case leads to long bonds and low bond orders. The importance of the  $\pi$ -acceptor ability of the carbene or silylene ligand in the formation of the multiple bond is therefore reinforced.

The CDA results are shown in Table 5. One of the

(48) Frenking, G. Personal communication, 1999.

(49) Arnold, F. P. Unpublished results.

(50) Novak, I.; Huang, W.; Luo, L.; Huang, H. H.; Ang, H. G.; Zybll, C. E. *Organometallics* **1997**, *16*, 1567.

Table 5. CDA Results

L	X	Si→Ru	Ru→Si	repulsion	$\lambda$	$E_{\text{snap}}$ (kcal/mol)
PH <sub>3</sub>	H	0.528	0.366	-0.204	0.041	82.6
PH <sub>3</sub>	Me	0.560	0.426	-0.251	0.046	81.2
PH <sub>3</sub>	SH	0.554	0.384	-0.223	0.033	79.0
PMe <sub>3</sub>	H	0.552	0.316	-0.193	0.034	86.8
PMe <sub>3</sub>	Me	0.483	0.308	-0.173	0.039	85.2
CO	H	0.410	0.307	-0.285	0.036	66.2
PH <sub>3</sub> <sup>a</sup>	CH <sub>2</sub>	0.423	0.283	-0.415	0.008	109.7

<sup>a</sup> Molecule is Cp(PH<sub>3</sub>)<sub>2</sub>Ru=CH<sub>2</sub><sup>+</sup>.

chief advantages of CDA is that it is correct only for complexes that are donor–acceptor complexes of the Dewar–Chatt–Duncanson type. All others possess large residuals and unphysical populations, which indicate the method is not appropriate. As may be seen from Table 5, all of the complexes have a small residual value, indicating that the DCD model is appropriate to some degree, although it should be noted that these residuals are an order of magnitude higher than those reported by Frenking in his study on tungsten–ethylene complexes.<sup>51</sup> The reported populations are low, with a maximum of just over half an electron being donated to the metal and frequently less than 0.4 electron being back-donated. The dithiolsilylene fragment has the worst donating ability (0.410 electron) and the second worst back-donation (0.307), second only to the carbene. The back-donation is highly affected by the choice of ligand at both the ruthenium and the silicon, with those possessing methyl groups at silicon being worse than those with hydrogens. The weak back-donation, with the maximum in the case of Cp(PMe<sub>3</sub>)<sub>2</sub>RuSiH<sub>2</sub><sup>+</sup>, is in accordance with the bond distances, electron densities, and charges discussed earlier and represents a delicate interplay between the Ru–Si distance, the electron accepting ability of the Ru fragment, and the electrophilicity of the silicon. Finally, bond energies are reported in the last column of Table 5. These are not actual bond strengths, but are what Ziegler calls  $E(\text{snap})$  energies,<sup>52</sup> i.e., the energy difference between the complex and two fragments that have not been allowed to relax into their preferred, free, configuration. Therefore, the trend is more important than the absolute value, but it should be noted that all of the bond energies are no more than approximately 80% of the Ru=C bond, and in the case of Si(SH)<sub>2</sub><sup>+</sup>, 60%. As expected, the dithiolsilylene species has the weakest bond, and it may be therefore inferred, the lowest degree of  $\pi$ -bonding. This may also be seen from the repulsive term, where it is the highest member of the RuSi series.

Since carbenes may exist in several resonance forms, only some possessing metal–ligand multiple bonds,<sup>53</sup> Natural resonance theory calculations were performed<sup>54</sup>

(51) Pidun, U.; Frenking, G. *Organometallics* **1995**, *14*, 5325. (b) Vyboshchikov, S. F.; Frenking, G. *Chem. Eur. J.* **1998**, *4*, 1428.

(52) (a) Ziegler, T.; Tschinke, V.; Ursenbach, C. *J. Am. Chem. Soc.* **1987**, *109*, 4825. (b) Ziegler, T.; Tschinke, V. In *Bonding Energetics in Organometallic Compounds*; Marks, T. J., Ed.; ACS Symposium Series 428; American Chemical Society, Washington, DC, 1990.

(53) Collman, J. P.; Hegedus, L. S.; Norton, J. R.; Finke, R. G. *Principles and Applications of Organotransition Metal Chemistry*; University Science Books: Mill Valley, CA, 1987; pp 120–129.

(54) (a) Glendening, E. D.; Weinhold, F. *J. Comput. Chem.* **1998**, *19*, 593. (b) Glendening, E. D.; Weinhold, F. *J. Comput. Chem.* **1998**, *19*, 610. (c) Glendening, E. D.; Weinhold, F. *J. Comput. Chem.* **1998**, *19*, 628. (d) Suidan, L.; Badenhop, J. K.; Glendening, E. D.; Weinhold, F. *J. Chem. Ed.* **1995**, *72*, 583.

Table 6. NRT Results

L	X	bond order	% covalent	% double bond
PH <sub>3</sub>	H	0.92	90	10
PH <sub>3</sub>	Me	1.92	54	80
PH <sub>3</sub>	SH	0.48	58	1
PMe <sub>3</sub>	H(0°)	1.34	69	41
PMe <sub>3</sub>	H(35°)	1.68	58	65
PMe <sub>3</sub>	Me	1.80	54	74
CO	H	1.77	50	76
PH <sub>3</sub>	CH <sub>2</sub> <sup>a</sup>	1.75	65	63

<sup>a</sup> Molecule is Cp(PH<sub>3</sub>)<sub>2</sub>Ru=CH<sub>2</sub><sup>+</sup>.

in which the configurations were iterated to self-consistency.<sup>55</sup> The salient features of these calculations are summarized in Table 6. In the case of the dithiolsilylene complex, structures possessing a Ru–Si single bond, a Si to S(1) double bond, and an Si–S(2) single bond (Figure 4) were the dominant configurations, with a weight of 23%. The next largest contributor was structures in which the Si was bonded to the sulfurs as above, but possessed a lone-pair in an sp hybrid orbital ( $\sigma$ -donor configuration) rather than being directly bonded to the Ru, at 17%. Configurations in which the Si p-orbital remained vacant single bonds to sulfur were observed were at 8% and 7% for the Si–LP and Si–Ru single-bonded case, respectively. Finally, two configurations totaling 10% were observed for the system in which Si was multiply bonded to one sulfur and singly bonded to the other and the  $\sigma$ -orbital was vacant, with the Ru center possessing an extra lone-pair. This accounts for 65% of the available configurations and all those with weights above 4%. In no configuration with a weight above 0.5% was any multiple bond between the Si and the Ru observed.<sup>56</sup> In contrast to this result, the alkyl- and hydrogen-substituted silylenes all showed resonance structures in which the dominant configuration possessed a silicon–ruthenium double bond, with a weight between 40% and 80% of the total. This is in direct contrast to the case of the Fischer carbenes, in which configurations of M=C–O<sup>−</sup> and M<sup>−</sup>–C=O character are both found. In the case of the ruthenium thiolsilylene, it is essentially frozen into a Ru–Si=S configuration.

The NRT results, shown in Table 6, also show that the bonding in these complexes, with the exception of Cp(PH<sub>3</sub>)<sub>2</sub>Ru=SiH<sub>2</sub><sup>+</sup>, is approximately 50% covalent, with ionic structures making up the balance. This is in line with the AIM results, which indicated that the interactions were generally of a closed shell nature and that the covalency of the bonds were low. The bond orders are of interest since the NRT method, which attempts to break the bonding down into ionic and covalent interactions, reports bond orders that are

(55) The NRT analysis on the complexes consisted of the following steps: First five trial structures were produced, each possessing a Si–Ru double bond, two Ru–P single bonds, and a free cyclopentadienyl fragment, differing only in the position of the double bonds in the Cp fragment. NRTMEM was increased to 50 (to allow more trial structures at the expense of the secondaries), NRTTHR was increased to 5 due to the strongly delocalized nature of the system, and NRTLST was set to 2, meaning to print all resonance structures with a weight of 2% or greater. Those structures were then used as the input to the calculation, and the process was repeated until the output structures were the same as the input structures.

(56) It should be noted that the NRT method considers each possible arrangement of the bonding manifold in the Cp–M moiety to be an individual resonance structure, leading to many 5-fold degenerate configurations. Hence the large number of low-weight configurations in this study.



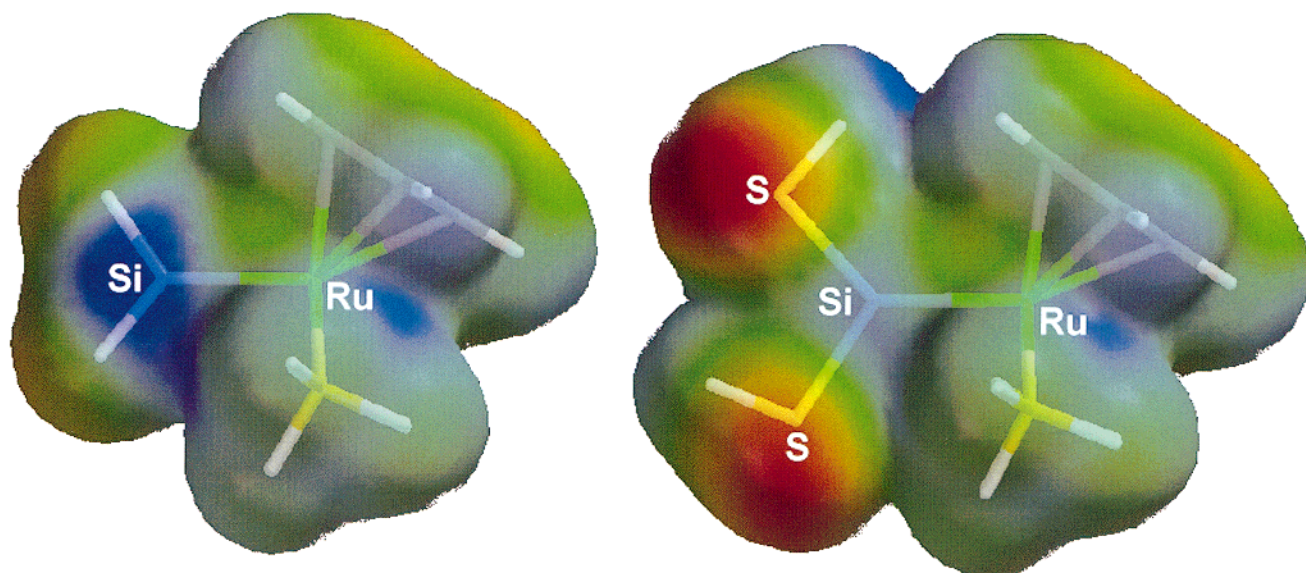


**Figure 5.** Electrostatic potential mapped onto 0.002 e/bohr<sup>3</sup> isosurface. Scale shown at left of image, blue regions are electrophilic (electron depleted), red are nucleophilic (electron rich), and green are neutral. The complexes shown are Cp(PH<sub>3</sub>)<sub>2</sub>RuSiH<sub>2</sub><sup>+</sup> (left) and Cp(PH<sub>3</sub>)RuSi(SH)<sub>2</sub><sup>+</sup> (right). Note the larger electrophilic region about the silicon in Cp(PH<sub>3</sub>)<sub>2</sub>RuSiH<sub>2</sub><sup>+</sup> vs Cp(PH<sub>3</sub>)<sub>2</sub>RuSi(SH)<sub>2</sub><sup>+</sup>. Images created with Spartan 5.1 (Wavefunction, Inc.) from Gaussian 94 (Gaussian Inc.) output files.

generally higher than those reported by the Wiberg or NLMO method. A bond order of nearly 2 was seen for most of the molecules, with the exception of the thiol-silylene, which had the lowest bond order at 0.48, and the dihydrosilylene fragment, which reported an order of 0.92. This is again in line with both the AIM results as well as contour plots of the  $\pi$ -orbitals of this system, which indicate a very weak  $\pi$ -interaction. The NRT results should be read with caution, since it has not been often applied to transition metal systems and has shown the tendency in the author's hands to fall into local minima, before true self-consistency is achieved. Despite these caveats, the data provided are consistent with those supplied by the other methods and assist in the interpretation of the bonding.

The Wiberg<sup>57</sup> and NLMO<sup>58</sup> bond orders are presented for comparison. They agree that the greatest degree of multiple bonding exists in the X = PMe<sub>3</sub>, Y = H complex, though they differ slightly with respect to the effect of the twist distortion. They are also much closer in magnitude to a single bond than a double, although they do generally indicate weak multiple-bond character. They are included only for comparative purposes, since they are often quoted in the literature.<sup>59</sup>

In Figure 5 may be seen a map of the electrostatic potential mapped onto the 0.002 au/bohr<sup>3</sup> isosurface<sup>60</sup> of Cp(PH<sub>3</sub>)<sub>2</sub>Ru=SiH<sub>2</sub><sup>+</sup> and Cp(PH<sub>3</sub>)<sub>2</sub>Ru=Si(SH)<sub>2</sub><sup>+</sup>.<sup>61</sup> The

unsubstituted silylene fragment possesses a strong electropositive character at the nucleus, indicating its electrophilic nature, while the dithiol-silylene has both a lower potential and strong nucleophilic character on the adjacent ligands. This explains the difficulty in isolating metal silylene complexes without base stabilization, since as the figure shows, the only other region of the molecule that possesses a similar electrophilic character is a strongly sterically hindered region opposite the Ru–Si bond.

## Discussion

The CpRu silylenes are computed to be mostly closed shell systems with dative Si→Ru  $\sigma$ -bonds and low Ru–Si  $\pi$ -back-bonding. The silicon is an electron-deficient center that is made more so by either electronegative substituents or competition with  $\pi$ -acid ligands on the ruthenium center. Evidence for this view is the low electron densities at the Ru–Si critical points, the low ellipticities, which are similar in magnitude to those observed for the Ru–P bonds, NBO and CDA results, and electrostatic potential maps. This leads to the conclusion that despite the electron-rich metal center present in Cp(PR<sub>3</sub>)<sub>2</sub>Ru, it is still difficult to force enough electron density onto the silicon to yield a good  $\pi$ -bond. This is not entirely unexpected, since it has been shown in other studies that alkylidene type ligands may become electrophiles, depending upon the environment about the metal. In metallocarbon chemistry, these are often cations,<sup>62</sup> a trend that is enhanced in the ruthenium silylenes by the more electropositive silicon ligand. This would suggest that a change of ligand set about the ruthenium, such as replacement of the Cp with a

(57) Wiberg, K. *Tetrahedron* **1968**, *24*, 1083.

(58) (a) Reed, A. E.; Schleyer, P. v. R. *Inorg. Chem.* **1988**, *27*, 3969. (b) Reed, A. E.; Schleyer, P. v. R. *J. Am. Chem. Soc.* **1990**, *112*, 1434.

(59) The NBO 4.0 manual clearly states that they are output simply because they are virtually free computationally, and often seen in the literature, but should not necessarily be trusted or believed. See ref 35 for further details, and Fenske, R. *Pure Appl. Chem.* **1988**, *60*, 1153, for further discussion of the hazards of the various population-based analysis methods.

(60) (a) Weiner, P. K.; Landridge, R.; Blaney, J. M.; Schaefer, R.; Kollman, P. A. *Proc. Natl. Acad. Sci. U.S.A.* **1982**, *79*, 3754. (b) Murray, J. S.; Politzer, P. *Chem. Phys. Lett.* **1988**, *152*, 364. (c) Bader, R. F. W.; Henneker, W. H.; Cade, P. E. *J. Chem. Phys.* **1967**, *46*, 3341.

(61) An isosurface is a continuous surface or envelope formed by connecting all points of a constant value.

(62) (a) Brookhart, M.; Tucker, J. R.; Husk, G. R. *J. Am. Chem. Soc.* **1983**, *105*, 258. (b) Hatton, W. G.; Gladysz, J. A. *J. Am. Chem. Soc.* **1983**, *105*, 6157. (c) Brookhart, M.; Kegley, S. E.; Husk, G. R. *Organometallics* **1984**, *3*, 650. (d) Casey, C. P.; Miles, W. H.; Tukada, H. *J. Am. Chem. Soc.* **1985**, *107*, 2924.

neutral ligand capable of donating six electrons, thereby creating a neutral rather than cationic complex, may have a salutary effect upon the bonding.

The observed bond distances show that there is a preference for aliphatic ligands as substituents on the phosphines, while the use of electron-withdrawing groups at silicon only strengthens the Si–X bond at the expense of the Si–Ru bond. In short, while some degree of multiple bonding exists in all of the observed systems, it is low enough in many cases that it would not be incorrect to better describe these bonds as “augmented single” bonds, in a manner similar to that reported for M–SiR<sub>3</sub> bonds by previous workers.<sup>63</sup>

This interpretation is tempered by the NRT results, in which it is seen that, except for the case of X = SH, a resonance structure possessing doubly bonded Si–Ru character is the single dominant configuration. As a result, the reported bond orders are higher than those reported by other methods. While the bond orders are higher, and should be interpreted cautiously,<sup>64</sup> the order of the degree of multiple bonding is consistent with the other results. The favored composition remains trialkylphosphine groups at the ruthenium center and hydrogens at the silicon as the configuration that leads to the highest degree of silicon–ruthenium bonding.

The observed twisted geometry of the experimentally classified systems deserves special mention. While in principle the twist could align the vacant p-orbital of the silylene fragment with the Ru–P bond, allowing for an increase in electron density and strengthening of the  $\pi$ -system, this does not sufficiently increase the stability of the bond to overcome the geometric liability of such a configuration. Furthermore, the population of the Si p-orbital decreases by 0.03 electron upon twisting. Therefore, it is probable that the twisted geometry is a result of the sterically demanding environment about the Ru center and not due to electronic effects. If anything, it is a destabilizing influence, indicating that one factor to be overcome is that of steric interference in the Si–Ru bonding. While bulky groups may offer protection from outside attack, they also cause the bond to distort in a fashion that further weakens an already weak  $\pi$ -system. This leads to the somewhat distressing interpretation that there may not be a good way to make

a strong ruthenium–silicon multiple bond and that other metals may have to be tried instead.

## Conclusion

In conclusion, the available data indicate that the best approach to forming silicon to ruthenium (and by extension other late metals) multiple bonds depends on three factors. One must keep electron-withdrawing substituents away from silicon, as well as  $\pi$ -donors, increase the electron density at the metal center until it is a net donor, and keep bulky ligands from interfering with the geometry at the metal center. Choosing the central metal and ligand set such that the resulting complex is not cationic should also help, substituting rhodium or rhenium for ruthenium, for instance. The author would therefore suggest that a complex with trialkyl phosphine groups and pentamethyl Cp at the metal center, and a silicon substituted by either boryl or silyl groups, would have the best chance of yielding a reasonably strong  $\pi$ -system. An interesting synthetic approach incorporating some of these ideas was the complex by Woo and co-workers that used dimethylsilylene coordinated to TPP (*meso*-tetra-*p*-tolylporphyrin) osmium.<sup>65</sup> This complex is on the right track, since the TPP ring is perpendicular to the metal–Si axis and therefore should not sterically interfere, but suffers from the coordination of a strong  $\pi$ -acceptor ligand to the metal. Preliminary calculations indicate that while there is little interaction between the silylene and the TPP ring, there is also little indication of a multiple bond, and the silicon remains stubbornly strongly electrophilic.<sup>66</sup> This would explain the observation that the coordinating solvent could not be removed under conditions that did not also destroy the complex.

Given the previously mentioned utility of these complexes, they should provide a challenging target for the experimentalist for the foreseeable future.

**Acknowledgment.** I would like to thank Arnold L. Rheingold and T. Don Tilley for helpful discussion, Frank Weinhold for his assistance with the NRT analysis, Paul Popelier for his assistance in interpreting some of the AIM results, and Advanced Research Systems at the University of Chicago for the computational resources used in this study.

OM990553M

(63) Berry, A. D.; Corey, E. R.; Hagen, A. P.; MacDiarmid, A. G.; Salfeld, F. E.; Wayland, B. B. *J. Am. Chem. Soc.* **1970**, *92*, 1940.

(64) As was noted earlier, there is a tendency for NRT to fall into local minima, and it has not been often applied to transition metal systems. Therefore these results should be viewed cautiously and considered to be of a qualitative nature.

(65) Woo, L. K.; Smith, D. R.; Young, V. G., Jr. *Organometallics* **1991**, *10*, 3977.

(66) Arnold, F. P. Unpublished results.